Poly(9-vinylcarbazole)/Silver Composite Nanotubes and Networks Formed at the Air–Water Interface

Chang-Wei Wang,[1] Guo-Qing Xin,[1] Yong-Ill Lee,[2] Jingcheng Hao,[1] Jianzhuang Jiang,[1] Hong-Guo Liu[1]

[1]*Key Laboratory for Colloid and Interface Chemistry of Education Ministry, Shandong University, Jinan 250100, China*
[2]*Department of Chemistry, Changwon National University, Changwon 641-773, Korea*

Received 14 July 2009; accepted 14 September 2009
DOI 10.1002/app.31443
Published online 1 December 2009 in Wiley InterScience (www.interscience.wiley.com).

ABSTRACT: Silver-nanoparticle-doped poly(9-vinylcarbazole) (PVK) nanocomposites were prepared via the reduction of Ag^+ ions and the self-assembly of PVK on $AgNO_3$ aqueous solution surfaces. The formed composite nanostructures depended strongly on the experimental temperature. Thick round disks of PVK surrounded by discrete Ag nanoparticles and/or with irregular holes formed at room temperature; nanotubes and micronetworks doped with Ag nanoparticles formed at about 30–40°C, and networks formed at higher temperature. Further investigation revealed that the nanotubes were transformed from thin round disks. The length of the PVK/Ag composite nanotubes were longer than 10 μm, and the average size of the embedded Ag nanoparticles was found to be about 3.5 nm. The composite networks were composed of round pores with diameters of several hundred nanometers and fine silver nanoparticles embedded in the thin polymer films that covered the pores. The formation of the nanotubes was a very interesting self-assembly phenomenon of the polymer at the air–water interface that has not been reported before. © 2009 Wiley Periodicals, Inc. J Appl Polym Sci 116: 252–257, 2010

Key words: nanocomposites; self-assembly; nanoparticles; thin films

INTRODUCTION

Recently, the fabrication of polymer nanostructures at the air–water interface has attracted much attention. Amphiphilic conjugated polymer,[1] linear,[2–6] and star-shaped[7] block copolymers have been fabricated into circular, rodlike, fibril, and long cylindrical aggregates, netlike and grid structures, hairlike and needlelike architectures, dendritic superstructures, and even labyrinth patterns at the air–water interface through the self-assembly of the polymer molecules. Meanwhile, circular aggregates of poly(9-vinylcarbazole) (PVK) have been assembled at the air–water interface, and the electrochemical properties have been investigated.[8–10]

PVK is a photoconductive semiconductor polymer that possesses a high glass-transition temperature and good processability. Because of its specific electric and optical properties and wide applications in microelectronics, the structure and properties, including the crystalline morphology,[11] conformation,[12] and emission properties,[13–16] of bulk PVK have been studied extensively. Recently, inorganic nanoparticle/PVK nanocomposites have aroused much attention because of their unique photoconductive and photorefractive properties, which show important applications in high-density optical storage, optical amplification, and dynamic image processing. The doped nanoparticles acted as photosensitizers, and PVK acted as a matrix and charge-transport species. Light-emitting diodes composed of the nanocomposites doped with europium,[17] iridium,[18] and ruthenium[19] complexes have been fabricated, and the photorefractive effect and photoconductivity of the composites doped with semiconductor nanocrystals[20–22] and metal nanoparticles[23] have been investigated.

Polymer nanostructures, such as nanotubes, nanocapsules, and honeycomb films, show a wealth of potential applications in optoelectronic devices, catalysis, medicine carries, and so on. Recently, the preparation and characterization of polymer nanotubes have attracted much attention. A lot of synthetic methods have been developed,[24] including traditional template methods with sacrificial nanorods[25] and nanotubes or microtubes[26] as hard templates, a soft supramolecular template method,[27] a template-free self-assembly method,[28] a self-rolled method,[29] and a modified electrospan method.[30]

Correspondence to: H.-G. Liu (hgliu@sdu.edu.cn).
Contract grant sponsor: National Natural Science Foundation of China (NSFC); contract grant number: 20873078.
Contract grant sponsor: National Basic Research Program of China 973 Program; contract grant number: 2009CB930103.

Many kinds of polymers, including conjugated polymers, polyelectrolytes, and even block copolymers, have been assembled into nanotubes. Very recently, PVK nanotubes doped with europium complex molecules were prepared with porous anodized alumina membranes as templates, and the energy transfer from PVK to Eu(III) and the emission properties of the composite nanotubes were investigated.[31] To our best knowledge, this was the first report on PVK nanotubes. On the other hand, a simple technique was developed to fabricate honeycomb-patterned thin films of polymers.[32] This method was based on the self-assembly of polymer molecules around hexagonal-patterned water droplets that were formed on the organic solution surface upon evaporation of the solvent when the organic solution was spread on a solid substrate under humid air.[33] Honeycomb-patterned films of various polymers have been fabricated by this approach, and these structures show novel properties and potential applications. For example, the ordered honeycomb structures of a light-emitting conjugate polymer enhanced photocurrent generation[34]; the honeycomb-patterned biodegradable polymer film was used as a scaffold for bone tissue engineering, on which hydroxyapatite was formed.[35] However, the honeycomb structures were mainly formed on solid substrates. Recently, an attempt was made to fabricate honeycomb structures on a water surface.[36] The honeycomb structures formed on the water surface could be transferred onto any substrate, which is useful for many applications and studies.

Here we report the fabrication of PVK/Ag nanostructures at the air–water interface through a one-step synthesis and assembly process. PVK nanotubes embedded with silver nanoparticles in the walls and networks were obtained under appropriate conditions. To the best of our knowledge, this is the first example of the preparation polymer nanotubes at the air–water interface. This study not only provided a new approach for the preparation of polymer nanotubes and honeycomb structures but also gave insight into the self-assembly behavior of polymer molecules at the air–water interface.

EXPERIMENTAL

Chemicals

PVK (weight-average molecular weight = 81,800) was purchased from Aldrich (St. Louis, MO). $AgNO_3$ (99.9%) was purchased from Shanghai Chemical Co. (Shanghai, China) and was used as received. Chloroform was an analytical agent. Highly purified water was used with a resistivity of 18.0 MΩ cm or greater.

Preparation and characterization of the nanostructures

The experiment was carried out as described next. A clean beaker with an inner diameter of 5.7 cm was filled with 10 mL of an aqueous solution of $AgNO_3$ with a concentration of 1×10^{-4} mol/L. A chloroform solution (68 μL) of PVK with a concentration of 0.046 mg/mL was spread on the aqueous solution surface by a microsyringe. When the organic solvent evaporated, a thin film was formed at the interface through a self-assembly process after 20 min. The mean area per repeat unit of PVK was calculated to be about 0.26 nm^2. The temperature of the subphase was controlled between 20 and 60°C, and the temperature of the spreading solution was controlled at 20°C, respectively. The thin films at the interface formed with a subphase temperature of 20°C were treated by formaldehyde gas for 24 h, and those formed with subphase temperatures of 20–60°C were illuminated with UV light (λ = 254 nm) for 1 min and then transferred onto Formvar-covered 230-mesh copper grids by the Langmuir–Schaefer method for investigation by transmission electron microscopy (TEM; JEM-100CXII, Jeol Ltd., Tokyo Japan) and high-resolution transmission electron microscopy (HRTEM; JEOL-2010).

RESULTS AND DISCUSSION

Nanostructures formed at room temperature

Round thick disks with various sizes ranging from 100 nm to several micrometers formed after the chloroform solution of PVK was spread onto the $AgNO_3$ aqueous solution surface. After formaldehyde gas treatment or UV irradiation at room temperature, silver nanoparticles appeared around the PVK disks to form a ring structure. Figure 1 shows the TEM micrographs of the formed nanostructures. It is very interesting to get a ring structure composed of discrete metal nanoparticles, and researchers have made great efforts to assemble these structures, such as rings composed of cobalt nanoparticles[37] and gold nanoparticles[38] and nanorods.[39] The formation of the round disks of PVK was attributed to the aggregation of PVK molecules at the air–water interface after the evaporation of chloroform because of the strong interactions between the molecules. It was reported that it is difficult for the rays to penetrate the thick plates.[40] So after reduction by formaldehyde gas or irradiation by UV light, the Ag^+ ions adsorbed on the periphery of the round disks were reduced to Ag atoms to form nanoparticles that were arranged around the disks, whereas the Ag^+ ions under the thick PVK disks could not be reduced.

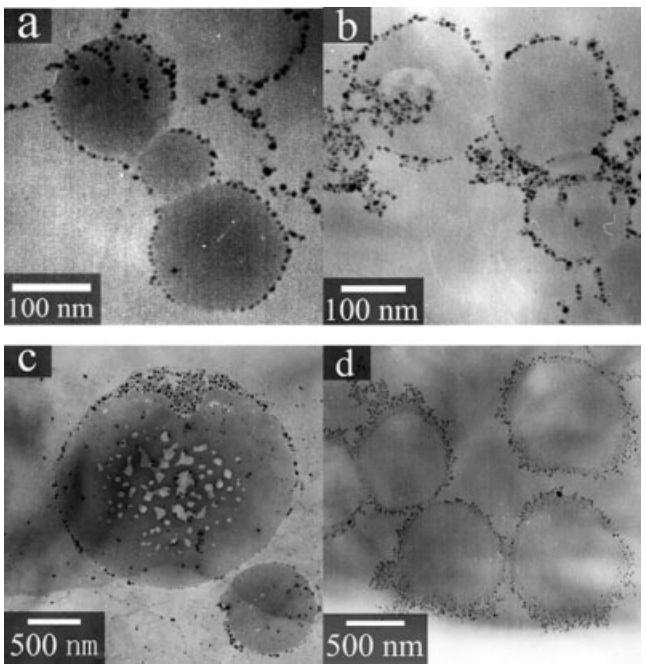

Figure 1 TEM micrographs of rings composed of Ag nanoparticles formed at room temperature by (a,b) formaldehyde gas treatment or (c,d) UV-light irradiation.

As shown in Figure 1(c), some irregular holes with different sizes appeared in the PVK disk. The network structure was much less than in the disks.

Nanostructures formed at higher temperatures

When the temperature of the subphase increased, instead of round thick disks, two kinds of nanostructures, that is, nanotubes and nanonetworks, appeared. Figure 2 shows the morphology of the nanotubes formed at 30, 32, and 35°C, respectively. The average outer and inner diameters and the wall thicknesses were 100–120, 80–90, and 15–20 nm, respectively, which were close to each other for the samples prepared under different subphase temperatures, and the length of the nanotubes reached several micrometers. The tubes showed two interesting features: (1) they had sharp, closed tips, and (2) the ends of some tubes connected with big round disks. Clearly, the tubes broke off from the center of the homogeneous disks that formed through the organization of the wires into a network, as seen from the periphery of the disks. This gave us a hint about the formation process of the nanotubes. First, a big,

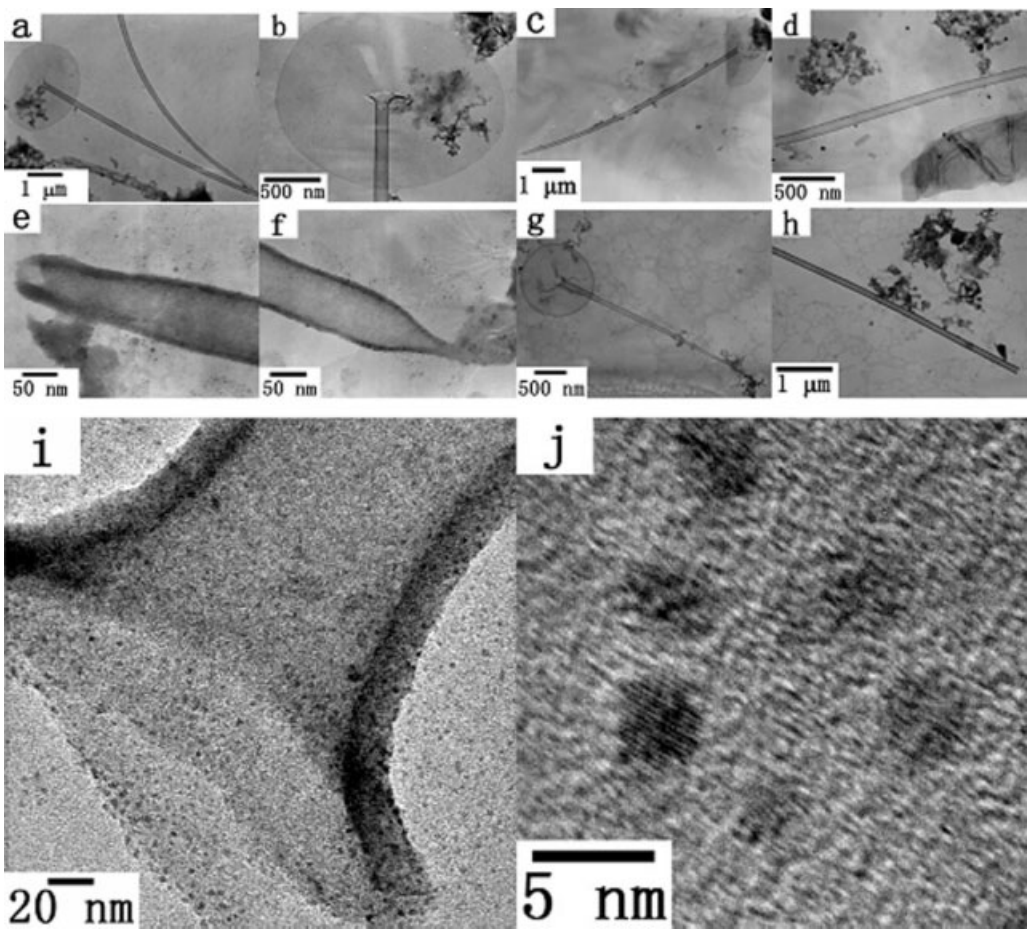

Figure 2 (a–i) TEM and (j) HRTEM micrographs of the PVK/Ag composite nanotubes formed at (a,b,i,j) 30, (c–f) 32, and (g,h) 35°C.

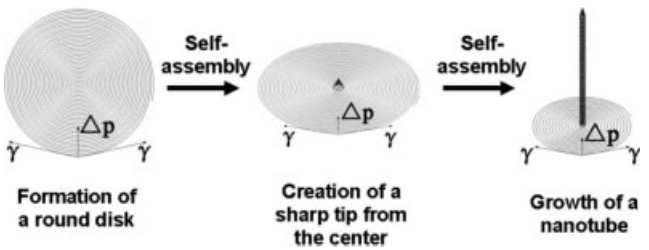

Scheme 1 Formation process of the nanotubes. γ represents surface tension and Δp represents additional pressure.

round thin plate formed at the air–water interface through a self-assembly process of the PVK chain and Ag^+ ions; then, a sharp tip of the nanotube protruded from the center of the plate; in the mean time, the plate shrank; this led to the creation of a nanotube. The nanotube grew to air straightly at the air–water interface. If the plate completely became nanotubes, the nanotube was down on the surface [Fig. 2(e,h)]; if the plate did not transform to nanotubes completely, there was a breakage between the end of the tube and the center of the plate, possibly because of the Langmuir–Schaefer transfer of the sample when the nanotube was growing (i.e., the copper grid pushed down the nanotube) or because of the overweight of the upstanding nanotube. The formation mechanism, which was similar to that of a single-walled carbon nanotube investigated *in situ* by TEM,[41] is illustrated in Scheme 1. Also, some nanoparticles were embedded in the walls of the tubes. During the formation process, Ag^+ ions were reduced to Ag atoms; this led to the generation of Ag nanoparticles embedded in the walls.

The particles dispersed on the walls showed a distinct lattice structure with an interplanar distance of 0.239 nm, which was close to 0.236 nm, with a lattice spacing between (111) facets of the face-centered cubic silver. The average diameter of the silver nanoparticles was about 3.5 nm. Smaller silver nanoparticles readily reacted with oxygen, transforming to Ag_2O and AgO upon exposure to air.[42,43] In our previous studies, we prepared silver nanoparticles with diameters of 3–5 nm at the air–water interface under Langmuir monolayers of *n*-hexadecyl dihydrogen phosphate.[44] The lattice spacing was found to be 0.265 nm, close to that between (111) facets of Ag_2O; this indicated that Ag nanoparticles transformed to Ag_2O ones after they were transferred to solid substrate and exposed to air. The silver nanoparticles that were embedded in the walls of the nanotubes were protected by the PVK molecules, which prevented the Ag nanoparticles from oxidation.

The formation of the nanotubes depended strongly on the experimental temperature. The temperature of the subphase was controlled at about 30–40°C. If the temperatures were too low, thicker plates formed. Under UV-light illumination for 1 min, fine nanoparticles were generated, which formed ringlike structures around the PVK plates (Fig. 1) because the UV light could not penetrate the thick plate to induce the formation of the Ag nanoparticles under the plate.[40] However, if the temperatures were too high, for example, at 45 and 55°C, just networks were observed, as discussed later. It was clear that the thickness of the plate had a great influence on the formation of the nanotubes. The driving force for the formation of the nanotube may have been the additional pressure (Δp) that came from the surface tension on the PVK plate edges and was directed to the center of the plate, as shown in Scheme 1. Of course, the interaction between the PVK molecules and water or Ag^+ ions in the subphase created a reaction force when the PVK plate shrank. As we know, the interaction between the PVK molecules and water was weaker because PVK is a hydrophobic molecule. So the nanotube formed when Δp was greater than the interaction. Thicker plates were too rigid to shrink. We drew the conclusion that only these plates with appropriate thickness (corresponding to the wall thickness) formed nanotubes through self-assembly process. This have been the reason why the nanotubes formed under different conditions had similar diameters and wall thicknesses.

From the view point of thermodynamics, we could explain the formation of the nanotube as follows. Let us consider a solid particle floating at the air–water interface. According to Young's formula, at a contact point between the water, solid particle, and gas phase, $\gamma_{gs} = \gamma_{ls} + \gamma_{gl} \cos \theta$, where γ_{gs}, γ_{ls}, and γ_{gl} refer to the interfacial surface energies of the gas–solid, water–solid, and gas–water interfaces, respectively, and θ refers to the contact angle. If $\theta > 90°$, $\gamma_{ls} > \gamma_{gs}$. PVK is a hydrophobic molecule; the water contact angle of PVK should be more than 90°. In our experiment, PVK molecules were spread onto water surface to form a thin layer with the help of chloroform. However, as discussed previously, $\gamma_{ls} > \gamma_{gs}$ for this system. So the PVK plate shrank to reduce the contact area between PVK and water. Meanwhile, the interfacial area between the gas and solid surface increased. Finally, the total energy decreased. In other words, this process took place spontaneously. On the basis of the analysis, we demonstrated that it was possible for such hydrophobic polymers as PVK and polystyrene to form nanotubes at the air–water interface. As for amphiphilic polymers, such as polystyrene-*block*-poly(ethyl oxide), or hydrophilic polymers, such as poly(methyl methacrylate), they could not form nanotubes by this method.

In addition to the nanotubes, nanonetworks appeared under the same experimental conditions,

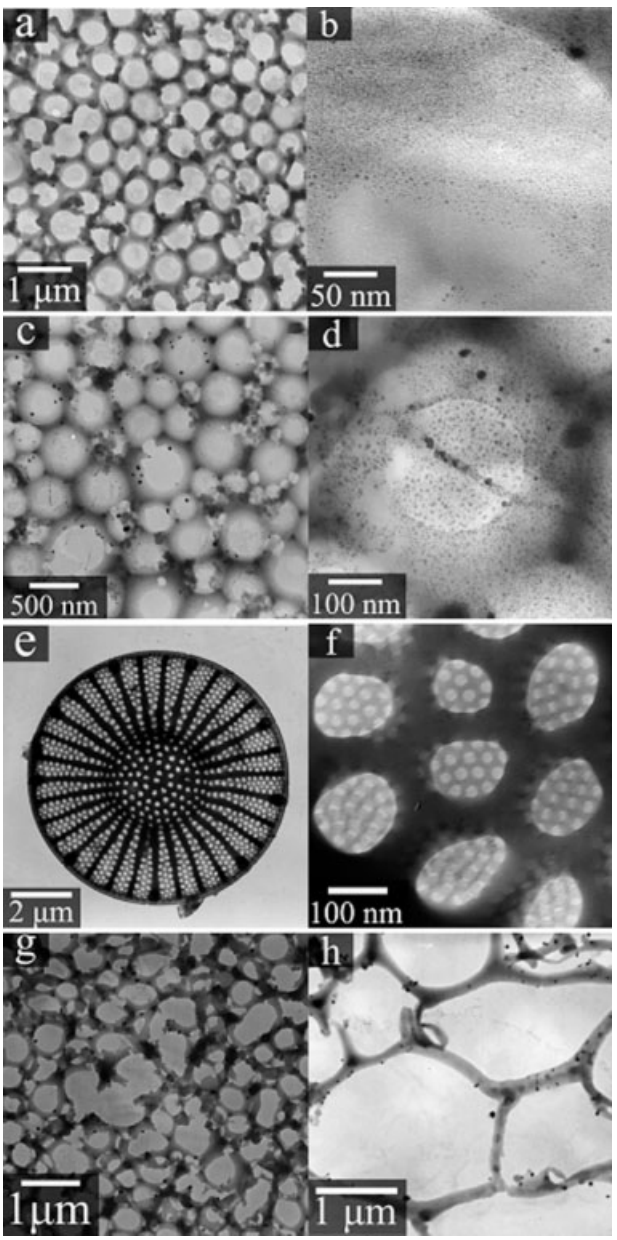

Figure 3 TEM micrographs of the PVK/Ag composite networks formed at (a,b) 32, (c–f) 38, (g) 45, and (h) 55°C.

as shown in Figure 3. The networks shown in Figure 3(a,c) were composed of closely packed round pores with diameters of several hundred nanometers. As shown in the enlarged micrographs in Figure 3(b,d), these pores were actually composed of thin PVK film embedded with fine nanoparticles, whose size increased with the subphase temperature. With increasing subphase temperature further, only network structures were observed; the pore size increased, the framework broke off, and larger silver nanoparticles appeared on the framework, as shown in Figure 3(e,f).

The formation of the honeycomb-like nanostructures shown in Figures 3(a–d) were ascribed to the condensed water droplets formed at the air–chloroform solution interface and the self-assembly of PVK molecules around the water droplets. The nucleation, growth, and coalescence of water droplets on the organic solution surface and the formation of ordered hexagonal arrays of water droplets depended on the experimental conditions, especially the relative humidity in the air. At lower temperatures, the relative humidity was lower, and the evaporation of chloroform was slower. Water droplets had difficulty forming on the organic solution surface under such conditions. On the other hand, the attraction between PVK molecules was stronger. This led to the formation of a large amount of round disks and several network plates with irregular holes (Fig. 1). With increasing subphase temperature, the relative humidity in air increased because of the evaporation of water, and the organic solvent evaporated rapidly, which led to a sharp decrease in the solution temperature on the solution surface, which benefited the nucleation, growth, and coalescence of water droplets on the solution surface. On the other hand, the attractive interaction between the PVK molecules weakened because of the thermal movement of the molecules under higher temperature. The honeycomb-like structures formed via the self-assembly of PVK molecules around the ordered arranged water droplets. The holes were covered with thin layers. This was similar to the honeycomb structure of poly(9,9′-dihexyfluorene) on solid substrates.[45] This indicated that the PVK thin films formed under such conditions could support the formed water droplets. Numerous fine silver nanoparticles were embedded in the thin layers, as shown in Figure 3(b,d).

When the subphase temperature increased further, the holes became larger and larger, the walls broke off, and big silver particles adsorbed on the walls. This was attributed to the increased relative humidity, the rapid evaporation of the solvent, and the violent thermal movement of the PVK molecules. With evaporation of chloroform, the temperature of the solution surface decreased sharply; this resulted in rapid nucleation, growth, and coalescence of the water droplets, which led to the creation of bigger droplets. At the same time, the film became too thin to support the droplets, and the viscosity of the organic solution became too low at higher temperatures; this led to the formation of void holes, as shown in Figure 3(g,h).

It should be noted that two kinds of nanostructures, that is, round disks and network structures appeared simultaneously at both room temperature or elevated temperatures. In fact, the nanotubes that arose from the big thinner round disks formed at higher temperatures. This may have been related to the spreading process of the organic solutions. As described in the Experimental section, the

chloroform solution of PVK spread dropwise onto the subphase surface with a limited area. In the early stage of spreading, the organic solution drop spread rapidly to form a thin layer on the subphase surface. The solvent evaporated so quickly that the water droplets could not form on the solution surface in time. The thin solid films formed and transformed to nanotubes at higher temperature because of the surface tension around the plates. When the water surface was occupied by the thin layers or nanotubes, the subsequent drops could not spread freely, the organic layers became thicker, and the evaporation time of the solvent became longer; this led to the nucleation and growth of water droplets on the solution surface. The polymer molecules self-assembled into solid structures after the complete evaporation of the solvent and water droplets. At last, the honeycomb-like structures formed.

CONCLUSIONS

In summary, we found for the first time that polymer nanotubes could be fabricated through a self-assembly process at the air–water interface. On the other hand, honeycomb-like nanostructures were fabricated at the air–water interface under humid air conditions, too. The formation of tubelike or honeycomb-like structures depended on the experimental conditions. This revealed the possibility to fabricate nanotubes without templates. This method could be extended to other polymer systems, and the formed nanotubes could conveniently be doped with other components, such as metal and semiconductor nanoparticles or functional molecules or metal complexes.

References

1. Kim, J.; McHugh, S. K.; Swager, T. M. Macromolecules 1999, 32, 1500.
2. Devereaux, C. A.; Baker, S. M. Macromolecules 2002, 35, 1921.
3. Cheyne, R. B.; Moffitt, M. G. Langmuir 2005, 21, 5453.
4. Zhang, J.; Cao, H.; Wan, X.; Zhou, Q. Langmuir 2006, 22, 6587.
5. Wen, G.; Chung, B.; Chang, T. Polymer 2006, 47, 8575.
6. Joncheray, T. J.; Denoncourt, K. M.; Meier, M. A. R.; Schubert, U. S.; Duran, R. S. Langmuir 2007, 23, 2423.
7. Gunawidjaja, R.; Peleshanko, S.; Genson, K. L.; Tsitsilianis, C.; Tsukruk, V. V. Langmuir 2006, 22, 6168.
8. Liu, J.-F.; Lu, Z.-H.; Yang, K.-Z. Thin Solid Films 1998, 322, 308.
9. Bertoncelloa, P.; Notargiacomob, A.; Nicolini, C. Polymer 2004, 45, 1659.
10. Hu, Z.-G.; Zhang, X.-T.; Dai, S.-X.; Cheng, G.; Li, Y.-C.; Du, Z.-L. Acta Chim Sin 2004, 62, 630.
11. Crystal, R. G. Macromolecules 1971, 4, 379.
12. Sundararajan, P. R. Macromolecules 1980, 13, 512.
13. Keyanpour-Rad, M.; Ledwith, A.; Johnson, G. E. Macromolecules 1980, 13, 272.
14. Johnson, G. E.; Good, T. A. Macromolecules 1982, 15, 409.
15. Molina, M. S.; Barrales-Rienda, J. M.; Riande, E.; Saiz, E. Macromolecules 1984, 17, 2728.
16. Evers, F.; Kobs, K.; Memming, R.; Terrell, D. R. J Am Chem Soc 1983, 105, 5988.
17. Yu, G.; Liu, Y.; Wu, X.; Zhu, D.; Li, H.; Jin, L.; Wang, M. Chem Mater 2000, 12, 2537.
18. Lee, C.-L.; Das, R. R.; Kim, J.-J. Chem Mater 2004, 16, 4642.
19. Xia, H.; Zhang, C.; Liu, X.; Qiu, S.; Lu, P.; Shen, F.; Zhang, J.; Ma, Y. J Phys Chem B 2004, 108, 3185.
20. Winiarz, J. G.; Zhang, L.; Lal, M.; Friend, C. S.; Prasad, P. N. J Am Chem Soc 1999, 121, 5287.
21. Wang, S.; Yang, S.; Yang, C.; Li, Z.; Wang, J.; Ge, W. J Phys Chem B 2000, 104, 11853.
22. Choudhury, K. R.; Samoc, M.; Patra, A.; Prasad, P. N. J Phys Chem B 2004, 108, 1556.
23. Kang, Y. O.; Choi, S.-H.; Gopalan, A.; Lee, K.-P.; Kang, H.-D.; Song, Y. S. J Appl Polym Sci 2006, 100, 1809.
24. Aleshin, A. N. Adv Mater 2006, 18, 17.
25. Mulvihill, M. J.; Rupert, B. L.; He, R.; Hochbaum, A.; Arnold, J.; Yang, P. J Am Chem Soc 2005, 127, 16040.
26. Tian, Y.; He, Q.; Cui, Y.; Tao, C.; Li, J. Chem—Eur J 2006, 12, 4808.
27. Gouet, J.; Samuel, J. D. J. S.; Kopyshev, A.; Santer, S.; Biesalski, M. Angew Chem Int Ed 2005, 44, 3297.
28. Zhang, Z.; Wei, Z.; Zhang, L.; Wan, M. Acta Mater 2005, 53, 1373.
29. Luchnikov, V.; Sydorenko, O.; Stamm, M. Adv Mater 2005, 17, 1177.
30. Li, D.; Xia, Y. Nano Lett 2004, 4, 933.
31. Moynihan, S.; Iacopino, D.; O'Carroll, D.; Doyle, H.; Tanner, D. A.; Redmond, G. Adv Mater 2007, 19, 2474.
32. Widawski, G.; Rawiso, B.; François, B. Nature 1994, 369, 387.
33. Karthaus, O.; Maruyama, N.; Cieren, X.; Shimomura, M.; Hasegawa, H.; Hashimoto, T. Langmuir 2000, 16, 6071.
34. Heng, L.; Zhai, J.; Zhao, Y.; Xu, J.; Sheng, X.; Jiang, L. Chem Phys Chem 2006, 7, 2520.
35. Tanaka, M.; Yoshizawa, K.; Tsuruma, A.; Sunami, H.; Yamamoto, S.; Shimomura, M. Colloids Surf A 2008, 313–314, 515.
36. Nurmawati, M. H.; Renu, R.; Ajikumar, P. K.; Sindhu, S.; Cheong, F. C.; Sow, C. H.; Valiyaveettil, S. Adv Funct Mater 2006, 16, 2340.
37. Tripp, S. L.; Dunin-Borkowski, R.; Wei, A. Angew Chem Int Ed 2003, 42, 5591.
38. Huo, Q.; Worden, J. G. J Nanoparticle Res 2007, 9, 1013.
39. Khanal, B. P.; Zubarev, E. R. Angew Chem Int Ed 2007, 46, 2195.
40. Chen, C.-Y.; Chen, C.-Y. Thin Solid Films 2005, 484, 68.
41. Hofmann, S.; Sharma, R.; Ducati, C.; Du, G.; Mattevi, C.; Cepek, C.; Cantoro, M.; Pisana, S.; Parvez, A.; Cervantes-Sodi, F.; Ferrari, A. C.; Dunin-Borkowski, R.; Lizzit, S.; Petaccia, L.; Goldoni, A.; Robertson, J. Nano Lett 2007, 7, 602.
42. Peyser, L. A.; Vinson, A. E.; Bartko, A. P.; Dickson, R. M. Science 2001, 291, 103.
43. Murakoshi, K.; Tanaka, H.; Sawai, Y.; Nakato, Y. J Phys Chem B 2002, 106, 3401.
44. Xiao, F.; Liu, H.-G.; Lee, Y.-I. Bull Korean Chem Soc 2008, 29, 2368.
45. Vamvounis, G.; Nyström, D.; Antoni, P.; Lindgren, M.; Holdcroft, S.; Hult, A. Langmuir 2006, 22, 3959.